AD-A100 263 ARMY ARMAMENT RESEARCH AND DEVELOPMENT COMMAND ABERD--ETC F/G 20/4
NONLINEAR VISCOELASTIC BREAKUP IN A HIGH-VELOCITY AIRSTREAM.(U)
MAR 81 J E MATTA
UNCLASSIFIED ARCSL-TR-80067 SBIE-AD-E410 398 NL

END
DATE FILMED
7 81
DTIC

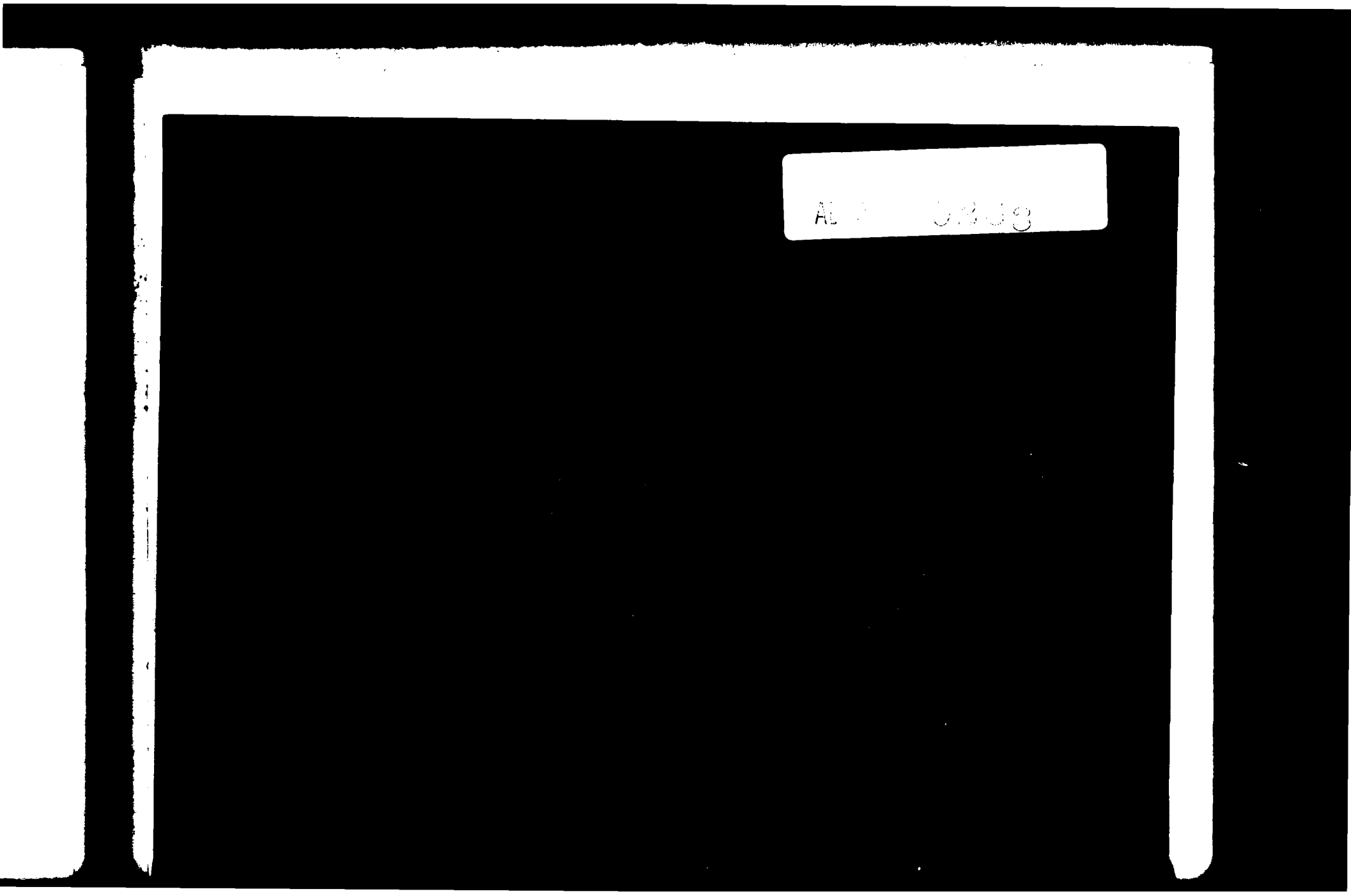

UNCLASSIFIED

SECURITY CLASSIFICATION OF THIS PAGE (When Data Entered)

REPORT DOCUMENTATION PAGE		READ INSTRUCTIONS BEFORE COMPLETING FORM
1. REPORT NUMBER ARCSL-TR-80067	2. GOVT ACCESSION NO. AD-A100263	3. RECIPIENT'S CATALOG NUMBER
4. TITLE (and Subtitle) NONLINEAR VISCOELASTIC BREAKUP IN A HIGH-VELOCITY AIRSTREAM		5. TYPE OF REPORT & PERIOD COVERED Technical Report May 1978—April 1980 6. PERFORMING ORG. REPORT NUMBER
7. AUTHOR(s) Joseph E. Matta, Ph.D.		8. CONTRACT OR GRANT NUMBER(s)
9. PERFORMING ORGANIZATION NAME AND ADDRESS Commander/Director, Chemical Systems Laboratory ATTN: DRDAR-CLB-PO Aberdeen Proving Ground, Maryland 21010		10. PROGRAM ELEMENT, PROJECT, TASK AREA & WORK UNIT NUMBERS 1L62706A553 Technical Area 3-4
11. CONTROLLING OFFICE NAME AND ADDRESS Commander/Director, Chemical Systems Laboratory ATTN: DRDAR-CLJ-R Aberdeen Proving Ground, Maryland 21010		12. REPORT DATE March 1981 13. NUMBER OF PAGES 30
14. MONITORING AGENCY NAME & ADDRESS(if different from Controlling Office)		15. SECURITY CLASS. (of this report) UNCLASSIFIED 15a. DECLASSIFICATION/DOWNGRADING SCHEDULE NA

16. DISTRIBUTION STATEMENT (of this Report)

Approved for public release; distribution unlimited.

17. DISTRIBUTION STATEMENT (of the abstract entered in Block 20, if different from Report)

18. SUPPLEMENTARY NOTES

19. KEY WORDS (Continue on reverse side if necessary and identify by block number)

Weber analysis	Wind tunnel experiment	Elvacite solution viscosity
Inviscid fluid	Diethylmalonate properties	Polymethylmethacrylate
Newtonian liquids	Polymer solution viscosities	Mass median diameters
Linear viscoelasticity	PMMA/Poly (ethyl/butylacrylate)	Jet analysis
Extensional viscosity		

20. ABSTRACT (Continue on reverse side if necessary and identify by block number)

Weiss and Worsham's predictions for atomization in high-velocity airstreams appear valid even when extended to higher viscosity fluids than originally derived. Newtonian, and viscoelastic fluids show different breakup mechanisms in high-velocity airstreams, as shown by injection photos, mass median diameters and drop-size distributions. Although not because of increase in viscosity alone, addition of polymer increases resultant particle size from liquids. For a given polymer, mass median diameter (MMD) versus λ correlation derived from Weber style analysis (using the conjectural elongational viscosity model) predicts performance when concentration is varied. The first normal stress difference measured for viscoelastic solutions correlated well with their dissemination performance (MMD).

DD FORM 1 JAN 73 1473 EDITION OF 1 NOV 65 IS OBSOLETE

UNCLASSIFIED

SECURITY CLASSIFICATION OF THIS PAGE (When Data Entered)

PREFACE

The work described in this report was supported by Project 1L162706A553, CB Defense & General Investigations; Technical Area 3-4, Operational Science/Technology. This work was started in May 1978 and completed in April 1980.

Acknowledgment

The author wishes to acknowledge the assistance of David Kimball and Robert Wright in assembling the wind tunnel and also of Raymond Tytus for measuring the rheological properties of the test fluids.

CONTENTS

NONLINEAR VISCOELASTIC BREAKUP IN A HIGH-VELOCITY AIRSTREAM

1. INTRODUCTION

Investigators[1-3] have shown that small additions of polymer to solutions may significantly alter their dissemination characteristics. Wilcox and Brown's study[1] of drop breakup in high-velocity airstreams has shown that it is possible to retard drop breakup by the addition of small quantities of polymer (as low as 0.1%) which impart viscoelasticity. Gerber and Stuempfle[2] have demonstrated, using an explosive projector system, that the generated particle size may vary considerably between liquids and suggested that this may result from the liquid exhibiting non-Newtonian characteristics when subjected to high transient stresses. Hoyt's photos[3] of jet discharges from a nozzle show differences in the surface appearance as it travels through the air and as it breaks up into a spray when small amounts of polymer are present. Although these studies qualitatively show that a slight addition of polymer significantly alters the deformation process, quantitative descriptions are not given.

To investigate the breakup behavior of viscoelastic fluids small quantities were injected into a high-velocity airstream. Rheological properties were varied to determine their effect on the resultant measured drop sizes. The breakup process was modeled using a Weber-style analysis in which only the simplest type of instability was considered: i.e., where the ligament necks off into a series of drops without interaction with the surrounding air.

2. WEBER-STYLE ANALYSIS

Weber's analysis of jets considers a long rod of liquid, of radius r_o, mass density ρ, and surface tension σ. The rod moves in the axial direction with a velocity V, and thus appears motionless in a coordinate system moving with this velocity. The surface tension causes the ligament to neck off into a series of drops. For a sufficiently low velocity ($We_a<4$)* one can neglect the interaction of the jet with the ambient air, and for Newtonian fluids this is the part of the theory that agrees best with experiment. A comprehensive review of Newtonian liquid jet breakup, however, is given by Reitz[4] where the wind inertia force is also considered. In this present viscoelastic-jet study even for $We_a>4$ the inertia effects of the air are neglected. For viscoelastic liquids the assumption perhaps is not too severe. The viscoelastic breakup photos (see figure 1) show no surface stripping even for large We_a indicating that perhaps the wind does not interact with the liquid aside from influencing the excess axial stress of the ligament.

---

*$We_a = D_o V^2 \rho_a/\sigma$, Weber number calculated using air density.

This observation is consistent with Hoyt's photos[3] which also show the elimination of small-scale surface disturbances upon slight additions of polymer to the fluid.

For a linearized-stability analysis, the disturbance is described by a small displacement U(x, t) in the axial direction, x. From mass conservation, the radius of the disturbed surface is $r_o\ (1 - \frac{1}{2} U_{,x})$.* The axial component of the momentum equation considering the radial stress due to surface tension is written as,

$$\rho U_{,tt} = -(\sigma/D_o)\ (U + r_o^2\, U_{,xx})_{,xx} + (S\,(U_{,x}))_{,x} \qquad (1)$$

The first group of terms on the right represents the axial pressure gradient caused by surface tension. $S(U_{,x})$ is the excess of axial tension over radial tension, produced by viscous, elastic, or other effects and is treated as linear function of $U_{,x}$. Considering solutions of the form $U(x, t) = U(t) \exp(i\zeta x/r_o)$ in equation (1) yields,

$$\theta^2\, U(t)_{,tt} = 4\zeta^2 \left\{(1-\zeta^2)\, U(t) - (D_o/\sigma)\, S(U)\right\} \qquad (2)$$

where

$D_o = 2r_o$, $\theta^2 = \rho D_o^3/\sigma$ and ζ is the wave number.

In most cases to be considered this equation is satisfied with

$$U(t) = U_o \exp(at) \quad \text{provided} \quad S(\exp(at)) = F(a) \exp(at).$$

F is a function of the growth rate, a, and independent of time, t. Then the momentum equation becomes

$$(\theta a)^2 = 4\zeta^2\{1 - \zeta^2 - (D_o/\sigma)\, F(a)\}. \qquad (3)$$

Although this linearized analysis is valid only for small disturbances it is assumed that the ultimate drop size is set by the wavelength of the fastest growing disturbance. Since solutions are of the form

$$U(x, t) = U(t) \exp(i\zeta x/r_o)$$

where

the wavelength of the disturbance L, is equal to $\pi D_o/\zeta$,

* Notation ,x implies differentiation with respect to x.

Figure 1. 9.8% Elvacite/Diethylmalonate Ejected into a High-Velocity Airstream

the volume of liquid in this length is $\pi r_o^2 L$ which results in a drop diameter,

$$D_{drop} = D_o\,(3\pi/2\zeta)^{1/3}. \tag{4}$$

Therefore the volume of the drop is determined from ζ corresponding to the fastest growing disturbance. Maximizing the secular equation (3) yields

$$\theta a = 2\zeta^2 \tag{5}$$

and

$$\theta a = 1 - (D_o/\sigma)\ F(a). \tag{6}$$

Since the drop volume is inversely proportional to ζ, the first relationship shows that anything that lowers the growth rate of the disturbance increases the drop volume. The result is independent of the fluid stress response. However, the second result shows that θa itself does depend upon the stress response of the material, since F(a) does. The following are a few examples of the resultant drop sizes for some of the various possible forms of F(a):

2.1 Case 1, Inviscid fluid:

For an inviscid fluid the excess stress,

$$S = 0 \ \therefore\ F(a) = 0.$$

As a result

$$\theta a = 1 \text{ and}$$

the maximum growth rate $a = 1/\theta$

so it is possible to consider θ as a characteristic breakup time for the inviscid case, and

$$\zeta = 2^{1/2}/2.$$

2.2 Case 2, Newtonian fluid:

For a Newtonian fluid the excess stress,

$$S = 3\eta U_{,xt} \ \therefore\ F(a) = 3\eta a$$

where

η is the shear viscosity.

Substituting into equation (6) and solving for θa yields,

$$\theta a = (1 + 3Z)^{-1}$$

where

$$Z, \text{ the Ohnesorge number, } = \eta/(D_o \rho \sigma)^{1/2}.$$

The viscosity lowers the growth rate and, thus, as is expected, increases the drop size. From equation (4),

$$D_{drop} = 1.88\ D_o\ (1 + 3Z)^{1/6}.$$

2.3 Case 3, Linear viscoelastic fluid:

For a linear viscoelastic fluid,

$$S = \int_{-\infty}^{t} 3G\ (t-t')\ U_{,xt}\ (t')dt$$

where

G(t) is the shearing stress relaxation modulus. Then,

$$F(a) = 3a\ \bar{G}(a)$$

where

$\bar{G}$ is the Laplace transform of G(t). For the simple case,

$$G(t) = G_o e^{-t/\lambda}$$

where

λ is the mean relaxation time of the fluid. The Laplace transform of equation (8) yields,

$$F(a) = 3a\eta/(1 + a\lambda).$$

This is the same form as the Newtonian case except that F(a) is decreased by factor $(1 + a\lambda)$ and thus the viscoelastic fluid behaves as a Newtonian fluid with reduced viscosity. Therefore smaller drops than a Newtonian liquid with the same steady-shearing viscosity are produced. The same is true for the more general case of G(t). This result is consistent with Middleman and Kroesser's observation[5] that the jet length is smaller for a viscoelastic fluid than for a Newtonian fluid with a similar Ohnesorge number. However, results of the experiment described below conducted at high relative wind velocities are contrary to this observation. The airstream, in fact, appears to stabilize the jet and thus produces larger drops.

2.4 Case 4, A conjectural model of extensional viscosity

Although the linearized analysis is not really applicable to the later stage of drop formation, one can obtain some idea of the nonlinear extensional viscosity effect if it is assumed that the linearized analysis is still applicable. Use of a formula derived for uniaxial extension from a convected-Maxwell constitutive relationship[6] yields for long times,

$$F(a) = 3\eta a / \{(1 - 2\lambda a)(1 + \lambda a)\}.$$

Again this result has the form of the Newtonian case, but F(a) is increased by a factor $1/(1 - 2\lambda a)$ thus the fluid behaves as a Newtonian fluid with an increased viscosity. The $1/(1 - 2\lambda a)$ term blows up when "a" approaches $1/2\lambda$, so the maximum growth rate is limited by $1/2\lambda$. Since λ is large in comparison to θ, it limits $a\theta$ to the small value $\theta/2\lambda$ and the corresponding wave number to $\zeta = 1/2\ (\theta/\lambda)^{1/2}$. By using the conjectural model of extensional viscosity one predicts a greater particle size than for the Newtonian case, and the drop volume should increase as $\lambda^{1/2}$ while the diameter increases as $\lambda^{1/6}$.

3. WIND TUNNEL EXPERIMENT

An experimental study to determine how rheological fluid properties affect the resultant drop size of a disseminated fluid was conducted by injecting a viscoelastic liquid into a large airstream of sustained high velocity. A "blow-down" wind tunnel was used to generate this high-velocity airstream. The tunnel consisted essentially of a 30-m^3 compression tank connected to a cylindrical test section (3-m long by 6.3-cm inside diameter) and then to an expansion section with a gradually increasing cross section. The fluid was injected coaxially with the wind about 2 m downstream of the compression tank. To inject the liquid, either a 0.30- or 0.46-cm-ID stainless steel tube was used, both having length-to-diameter ratio greater than 80. The disseminated drops were sampled on a vertical grid located in the expansion section of the tunnel. The cross

section of the paper-coated plywood grid was about 20% of the expansion section at the sampling location. The collected stains were measured on a Quantimet 720 Image Analyzer* and were converted to actual drop diameters by applying a previously calculated spread factor. (Glycerol drops were collected on teflon slides so actual distorted-drop-diameter measurements were made rather than stain measurements.) The relative airstream velocity measured with a Pitot tube was about 200 m/sec. A more detailed description of the tunnel and sampling technique is planned in another report.

4. TEST FLUIDS

The test fluids used in this study are shown in table 1 with some of their physical properties. Gaskins, F. H. et. al., in an unpublished CSL report, Rheology and Fluid Dynamics Studies of Thickened Liquid Chemical Agent Simulants, March 1978, is the source of the information. Diethylmalonate (DEM) is the solvent for the polymer solutions. The viscosity and first normal stress differences of the solutions were measured on a model 18 Weissenberg Rheogoniometer (appendix, figures A-1 and A-2). The polymer solutions are obviously viscoelastic while the DEM and glycerol fluids were Newtonian over this same range in shear rates with viscosities of 0.02 and 9.5 poise, respectively.

5. NEWTONIAN TEST RESULTS

Figure A-3 is a log probability curve of the measured particle diameters for the glycerol disseminated in the high-velocity wind tunnel. The plot indicates that the droplets are essentially log normally distributed although the slight inflection hints that the distribution is slightly bimodal.[7] Table 2 shows that the measured mass median diameter (MMD) agrees well with the empirical prediction of Weiss and Worsham obtained for low viscosity fluids.[8]

Weiss and Worsham results were correlated empirically by

$$(X\rho_a V^2/\sigma) = .61(V\eta/\sigma)^{2/3}\,(1 + 10^3\rho_a/\rho)\,(W\rho\sigma\eta_a/\eta^4)^{1/2}$$

where mass median diameter X, air density (ρ_a), relative velocity (V), liquid viscosity (η) and mass injection rate (W) were changed over 4-to-25-fold range. Surface tension (σ), liquid density (ρ), and air viscosity (η_a) were not varied significantly.

*Manufactured by Cambridge Instruments, Monsey, New York.

Table 1. Physical Chemistry Data

A. Pure Liquids

Property	DEM	Glycerol
Surface Tension dyne/cm	30.4 (@30°C)	63.0 (@30°C)
Density, gm/cc	1.05 (@25°C)	1.26 (@30°C)
Viscosity, poise	.02 (@21°C)	9.0 (@21°C)

B. DEM Polymer Solutions

Type	Molecular weight (viscosity-avg.)	Concentration	Zero shear viscosity
		%	poise
Polymethyl-methacrylate (PMMA)	6×10^6	2.1	100.
		1.5	16.
		1.0	2.0
		0.5	0.3
Copolymer 80% PMMA 20% Polyethyl/-butyl-acrylate	1.9×10^6	5.2	9.0
Elvacite	4.0×10^5	9.8	9.5

Table 2. Comparison of the MMD Test Results Versus the Weiss and Worsham Predictions. Both the standard errors and deviations (terms in parentheses) are shown for the measured results.

FLUID	Drop Diameter, microns	
	Weiss & Worsham	Measured
2.1% Poly(methylmethacrylate) /diethylmalonate (PMMA/DEM)	210	1980 ± 250 (400)
1.5% PMMA/DEM	110	1780 ± 200 (250)
1.0% PMMA/DEM	60	1480 ± 150 (250)
0.5% PMMA/DEM	30	1050 ± 150 (300)
5.2% Copolymer/DEM	100	1300 ± 150 (200)
9.8% Elvacite/DEM	100	1300 ± 150 (250)
DEM	10	Too small to measure
Glycerol	130	160 ± 20 (30)

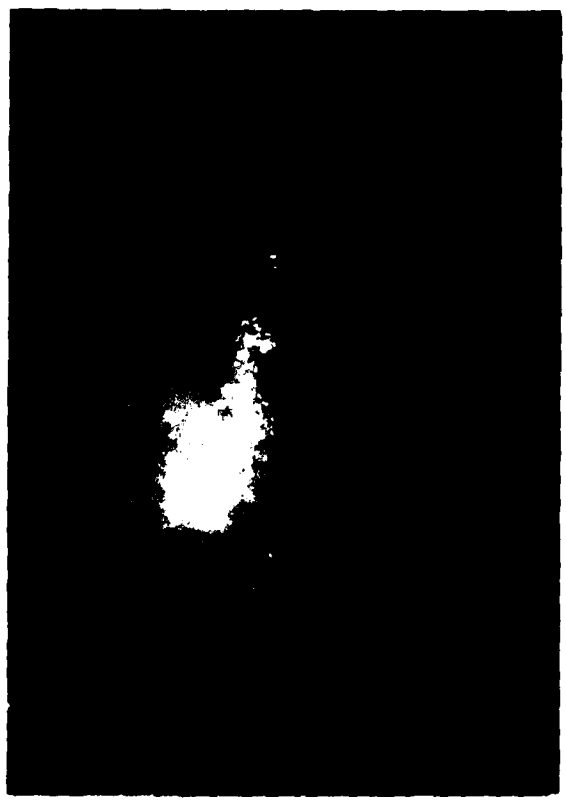

Figure 2. Glycerol Ejected into a High-Velocity Airstream

It was not possible to measure the MMD for the neat DEM since the disseminated particles were too small to measure using this technique.

To observe the dissemination behavior of the fluids photos using a high-intensity strobe light were taken of the fluid ejecting from the nozzle. Figure 2 clearly shows the rapid atomization that occurs for glycerol in the high-velocity airstream near the nozzle exit.

6. VISCOELASTIC RESULTS

The normally distributed disseminated 9.8% Elvacite fluid is clearly evident from the linear probability fit (figure A-4) of four combined-replica tests. Similar distributions were observed for the other polymer solutions as well. The breakup behavior of the viscoelastic fluid as it is ejected from the nozzle (figure 1) obviously differs from that of the Newtonian fluid. The fluid appears very stable and does not atomize rapidly as does the Newtonian liquid which eventually results in different final drop sizes.

Shown in table 2 are the measured MMD's for the polymer solutions tested. The measured particle sizes are an order of magnitude larger than that predicted from the Weiss and Worsham equation. Actually the difference is possibly even greater since zero shear viscosity values were used in the calculation rather than the lower values that exist within the injection tube. A comparison with the glycerol results indicates that viscosity can not account for increased particle size.

7. DISCUSSION

Breakup of the viscoelastic fluids occurred between 0.2 and 2.0 meters downstream of the nozzle. The corresponding process breakup times as estimated from the breakup distance and average airspeed are about 1.0 and 10 msec. Assuming the deformation rate is inversely proportional to the process time results in a deformation rate ranging from 1000 to 100/sec. Thus attempts to correlate MMD's were based on rheological properties measured at a shear rate of 500/sec.

To test the predicted correlation of the Weber analysis (case 4), a plot of the MMD's of the disseminated polymer solutions versus λ was made (figure A-5). The relaxation time of each fluid was calculated using the relationship $\lambda = N_1/\tau\dot{\gamma}$ where N_1, and the shear stress, τ, are measured at the same shear rate, $\dot{\gamma} = 500/\text{sec}$. MMD data for the four PMMA solutions correlated well with λ, but when one varies the polymer a single correlation does not exist. This deficiency is possibly due to a single rather than

a spectrum of relaxation times associated with the conjectured extensional viscosity model. Spectrum extensional models heavily weight the larger relaxation times while steady shear experiments tend to be insensitive to the upper portion of the spectrum.[6] Thus a mean relaxation time calculated from the shear experiment is not appropriate when one considers solutions where the polymer and therefore molecular weight distribution differ.

A good correlation for all the polymer results was found with the first normal stress difference measured at 500/sec (figure A-6). Whether this correlation is fortuitous or not is uncertain. However, it is not too surprising since N_1 is an indication of the elastic nature of the fluid. Proposed-elongational-viscosity measurements using a bubble collapse technique[9] should elucidate this concern.

A linear relationship between the MMD and injection-tubing inside diameter is also shown in figure A-6. This is expected from the Weber analysis since the final drop size is proportional to the initial jet diameter (equation 4).

8. CONCLUSIONS

1) The Weiss and Worsham empirical relationship appears valid even when extended to higher viscosity fluids than for which it was originally derived.

2) The breakup mechanism in a high-velocity airstream is different for Newtonian and viscoelastic fluids as is evident from the comparative injection photos, resultant MMD's and final drop-size distribution data.

3) Addition of polymer increases the resultant particle size but this increase is not solely due to the increase in the liquid's viscosity.

4) The MMD versus λ correlation derived from the Weber style analysis using the conjectured-elongational-viscosity model was found to predict performance when the polymer concentration (but not type) was varied.

5) The first normal stress difference measured for viscoelastic solutions correlated well with their dissemination performance (MMD).

LITERATURE CITED

1. Wilcox, J. D., June, R. K., and Brown, H. A. The Retardation of Drop Breakup in High-Velocity Airstreams by Polymeric Modifiers. J. of Appl. Polym. Sci., 5(13), 1-6 (1961).

2. Gerber, B. V. and Stuempfle, A. K. Proceedings of the 1976 Army Science Conference United States Military Academy, West Point, New York, 22-25 June 1976. A New Experimental Technique for Studying the Explosive Communition of Liquids (U). TDS 004.7-11/Vol 1, (1976). August 1976.

3. Hoyt, J. W., Taylor, J. J. and Runge, C. D. The Structure of Jets of Water and Polymer Solution in Air. J. Fluid Mech, 63 (11), 635-640 (1974).

4. Reitz, R. D. Atomization and Other Breakup Regimes of a Liquid Jet. Princeton University, PhD Dissertation, 1978.

5. Middleman, S., and Kroesser. Viscoelastic Jet Stability. AIChE J. 15 (3), 383-368 (1969).

6. Denn, M. M. Extensional Flows Experiments and Theory, 1977 Joint Applied Mechanics, Fluids Engineering and Bio Engineering Conference, Yale University, June 15-17, 1977.

7. Gerdan, G. Small Particle Statistics. Academic Press, 2nd Edition, New York, New York, 96-97 (1960).

8. Weiss, M. A., and Worsham, C. H. Atomization in High Velocity Airstreams. ARS J. 29, 252 (1959).

9. Pearson, G. and Middleman, S. Elongational Flow Behavior of Viscoelastic Liquids: Part I Modeling of Bubble Collapse. AIChE J. 23 (5), 714-722 (1977).

APPENDIX

FIGURES

(PLOTS)

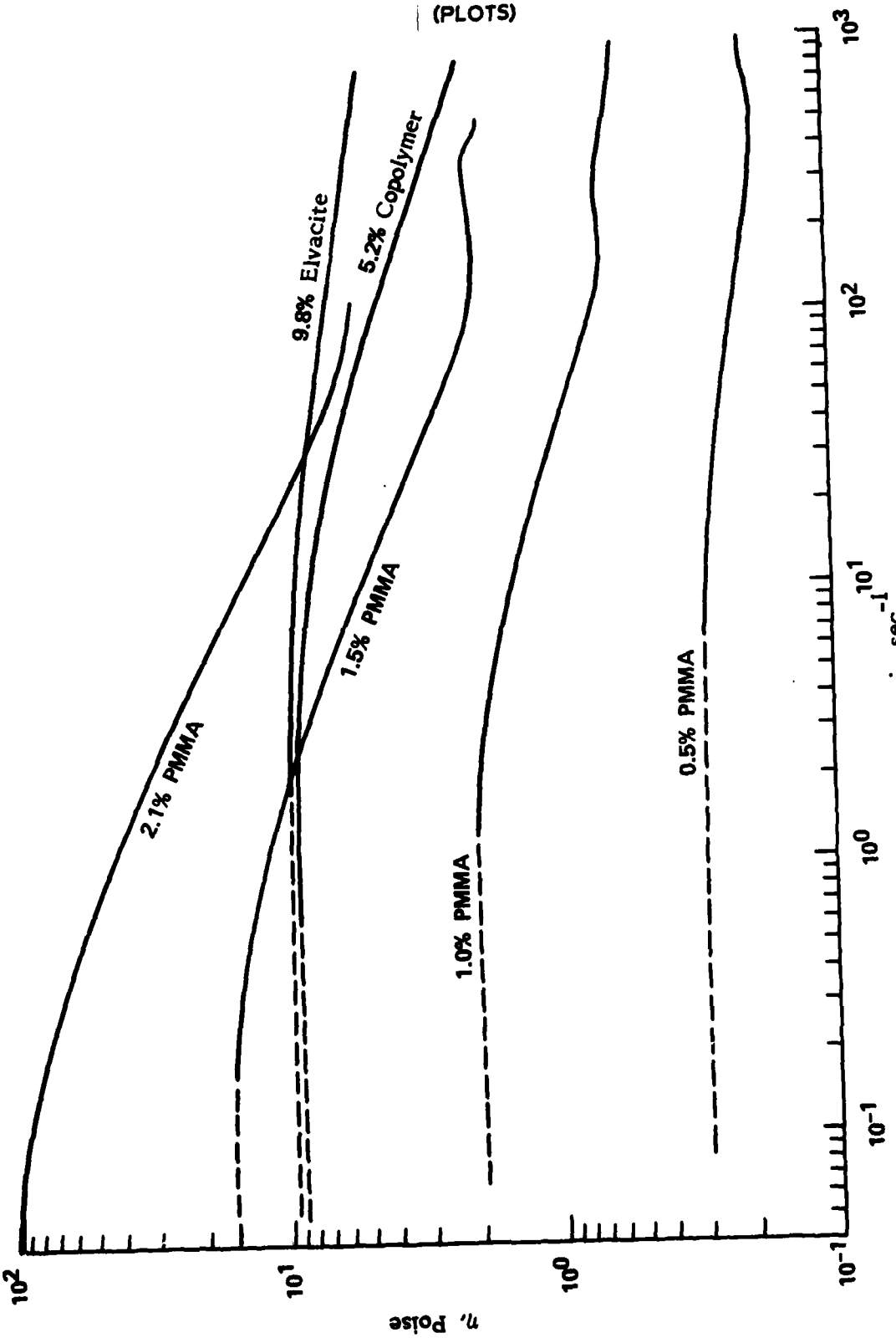

Figure A-1. Viscosity Measurements Versus Shear Rate for Polymer Test Solutions. Dashed lines are extrapolated zero shear viscosity values.

Figure A-2. Cone and Plate First Normal Stress Measurements for Polymer Test Solutions

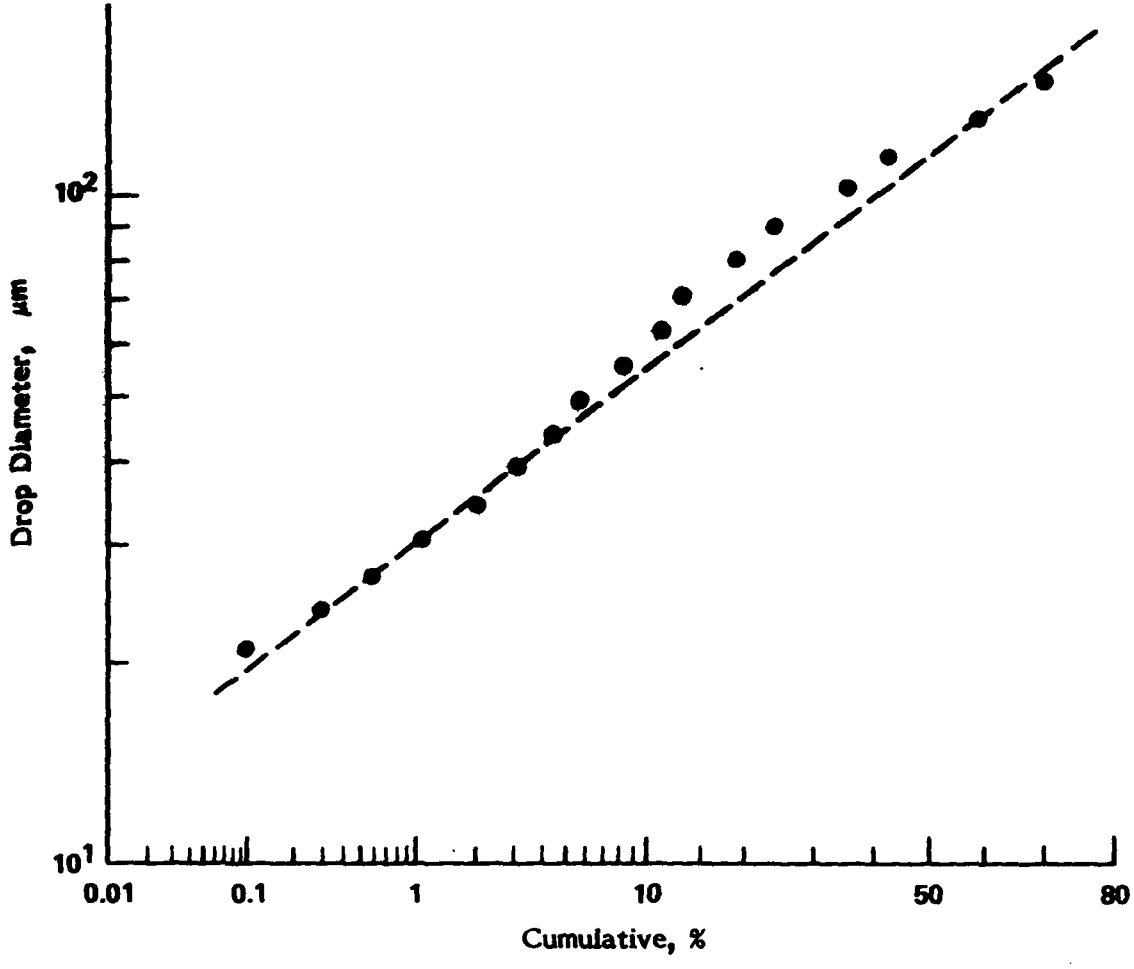

Figure A-3. Cumulative Mass-Log-Normal-Probability Plot for the Glycerol Test Results

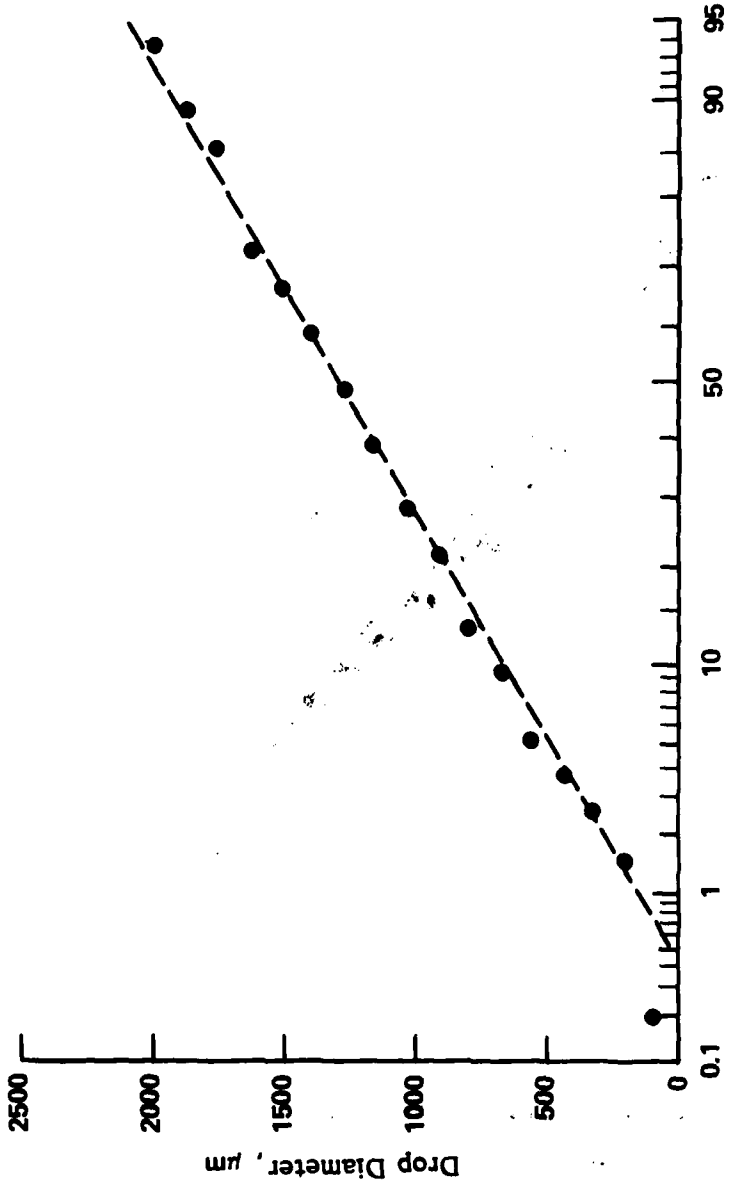

Figure A-4. Cumulative Mass-Normal-Probability Plot for Four Replica 9.8% Elvacite/DEM Test Results

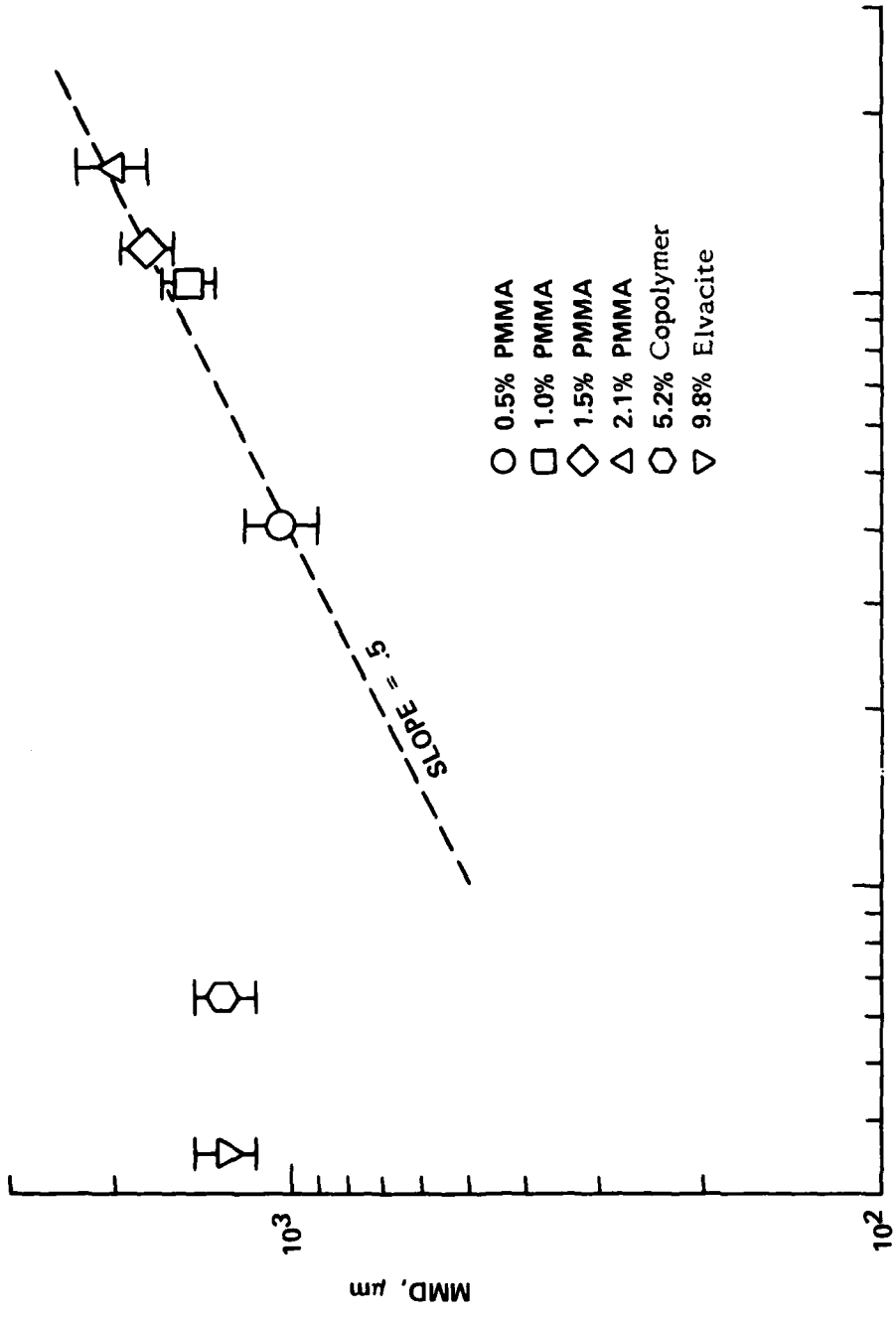

Figure A-5. Test Results, Mass Median Diameter, Versus Relaxation Times Calculated at 500 sec^{-1}

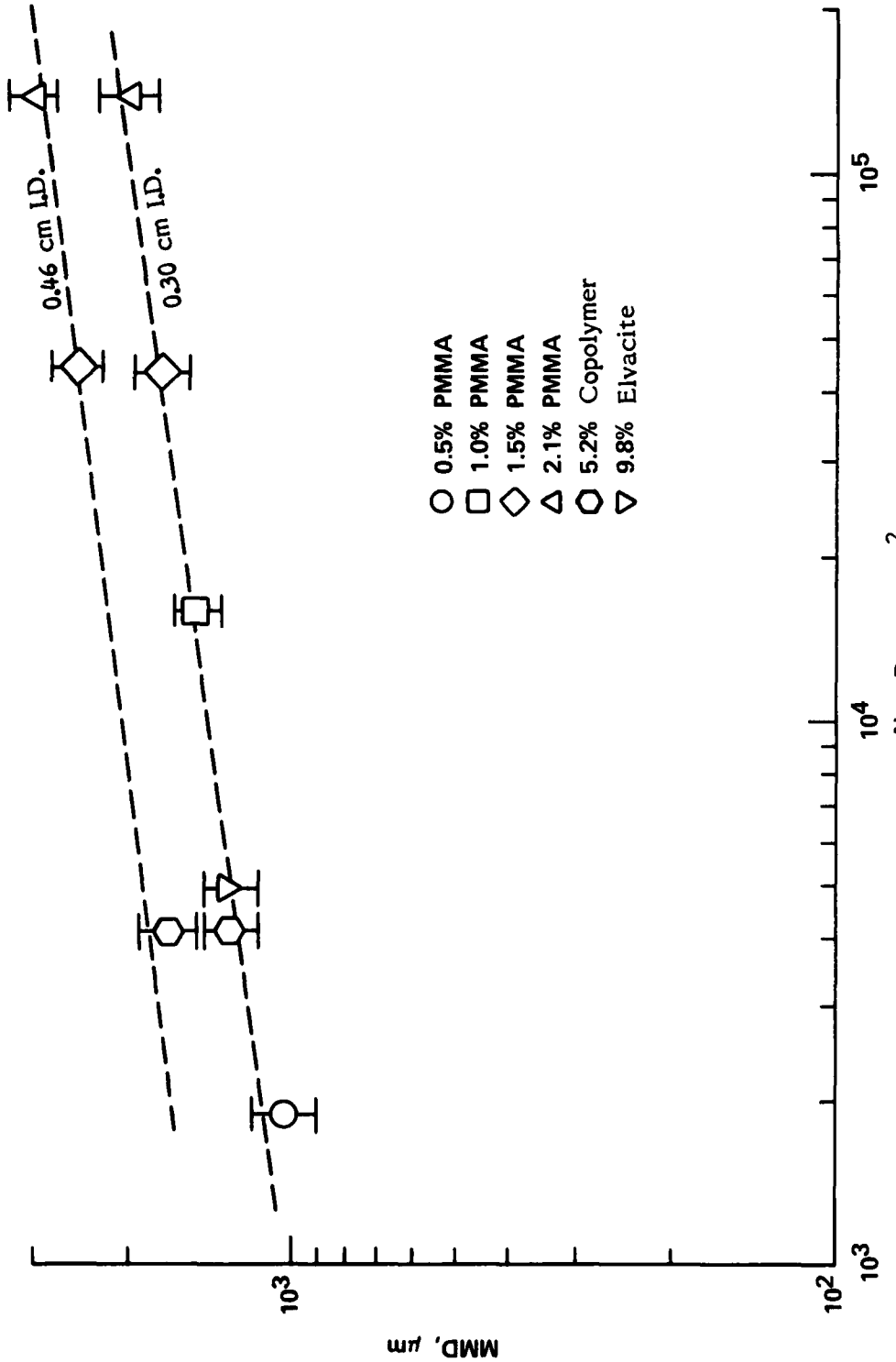

Figure A-6. Test Results, Mass Median Diameter, Versus First Normal Stress Difference Measured at 500 sec^{-1}

DISTRIBUTION LIST 3

Names	Copies
CHEMICAL SYSTEMS LABORATORY	
ATTN: DRDAR-CLF	1
ATTN: DRDAR-CLJ-R	3
ATTN: DRDAR-CLJ-L	3
ATTN: DRDAR-CLJ-M	1
ATTN: DRDAR-CLJ-P	1
ATTN: DRDAR-CLT	1
ATTN: DRDAR-CLN	1
ATTN: DRDAR-CLB-C	1
ATTN: DRDAR-CLB-P	1
ATTN: DRDAR-CLB-PA	1
ATTN: DRDAR-CLB-PO	1
ATTN: DRDAR-CLB-R	1
ATTN: DRDAR-CLB-TE	1
ATTN: DRDAR-CLY-A	1
ATTN: DRDAR-CLY-R	6
ATTN: DRDAR-CLR-I	1
ATTN: DRDAR-QAC-E	1
COPIES FOR AUTHOR(S) Research Division	15
DEPARTMENT OF DEFENSE	
Defense Technical Information Center ATTN: DTIC-DDA-2 Cameron Station, Building 5 Alexandria, VA 22314	12
Director Defense Intelligence Agency ATTN: DB-4G1 Washington, DC 20301	1
Special Agent in Charge ARO, 902d Military Intelligence GP ATTN: IAGPA-A-AN Aberdeen Proving Ground, MD 21005	1
Commander SED, HQ, INSCOM ATTN: IRFM-SED (Mr. Joubert) Fort Meade, MD 20755	1
DEPARTMENT OF THE ARMY	
HQDA (DAMO-NCC) WASH DC 20310	1
Deputy Chief of Staff for Research, Development & Acquisition ATTN: DAMA-CSS-C ATTN: DAMA-ARZ-D Washington, DC 20310	1 1
US Army Research & Standardization Group (Europe) ATTN: DRXSN-E-SC LTC J.M. Dorrance Box 65, FPO New York 09510	1
HQDA (DAMI-FIT) WASH, DC 20310	1
Commander HQ 7th Medical Command ATTN: AEMPM APO New York 09403	1
Commander DARCOM, STITEUR ATTN: DRXST-STI Box 48, APO New York 09710	1
Commander USAOTEA ATTN: CSTE-ZX 5600 Columbia Pike Falls Church, VA 22041	1
Commander US Army Science & Technology Center-Far East Office ATTN: MAJ Borges APO San Francisco 96328	1
Commander 2d Infantry Division ATTN: EAIDCOM APO San Francisco 96224	1
Commander 5th Infantry Division (Mech) ATTN: Division Chemical Officer Fort Polk, LA 71459	1

OFFICE OF THE SURGEON GENERAL

Commander
USA Biomedical Laboratory
ATTN: SGRD-UV-L 1
Aberdeen Proving Ground, MD 21010

US ARMY HEALTH SERVICE COMMAND

Superintendent
Academy of Health Sciences
US Army
ATTN: HSA-CDH 1
ATTN: HSA-IPM 1
Fort Sam Houston, TX 78234

US ARMY MATERIEL DEVELOPMENT AND READINESS COMMAND

Commander
US Army Materiel Development and Readiness Command
ATTN: DRCLDC 1
ATTN: DRCSF-P 1
5001 Eisenhower Ave
Alexandria, VA 22333

Director
Human Engineering Laboratory
ATTN: DRXHE-SP (CB Defense Team) 1
Aberdeen Proving Ground, MD 21005

Commander
US Army Foreign Science and Technology Center
ATTN: DRXST-MT3 1
220 Seventh St., NE
Charlottesville, VA 22901

Director
US Army Materiel Systems Analysis Activity
ATTN: DRXSY-MP 1
ATTN: DRXSY-T (Mr. Kaste) 1
Aberdeen Proving Ground, MD 21005

Commander
US Army Missile Command
Redstone Scientific Information Center
ATTN: DRSMI-RPR (Documents) 1
Redstone Arsenal, AL 35809

Director
DARCOM Field Safety Activity
ATTN: DRXOS-C 1
Charlestown, IN 47111

Commander
US Army Natick Research and Development Command
ATTN: DRDNA-O 1
ATTN: DRDNA-VC 1
ATTN: DRDNA-VCC 1
ATTN: DRDNA-VM 1
ATTN: DRDNA-VR 1
ATTN: DRDNA-VT 1
Natick, MA 01760

US ARMY ARMAMENT RESEARCH AND DEVELOPMENT COMMAND

Commander
US Army Armament Research and Development Command
ATTN: DRDAR-LCA-L 1
ATTN: DRDAR-LCM-E
ATTN: DRDAR-LCU 1
ATTN: DRDAR-LCU-CE 1
ATTN: DRDAR-PMA (G.R. Sacco) 1
ATTN: DRDAR-SCM 1
ATTN: DRDAR-TSS 2
ATTN: DRCPM-CAWS-AM 1
ATTN: DRCPM-CAWS-SI 1
Dover, NJ 07801

Director
Ballistic Research Laboratory
ARRADCOM
ATTN: DRDAR-TSB-S 1
Aberdeen Proving Ground, MD 21005

Commander
USA Technical Detachment 1
US Naval EOD Facility
Indian Head, MD 20640

US ARMY ARMAMENT MATERIEL READINESS COMMAND

Commander
USA ARRCOM
ATTN: SARTE 1
Aberdeen Proving Ground, MD 21010

Commander
US Army Armament Materiel
Readiness Command
ATTN: DRSAR-ASN 1
ATTN: DRSAR-IRC 1
ATTN: DRSAR-LEP-L 1
ATTN: DRSAR-PE 1
ATTN: DRSAR-SF 1
ATTN: DRSAR-SR 1
Rock Island, IL 61299

Commander
US Army Dugway Proving Ground
ATTN: Technical Library
Docu Sect 1
Dugway, UT 84022

US ARMY TRAINING & DOCTRINE COMMAND

Commandant
US Army Infantry School
ATTN: NBC Division 1
Fort Benning, GA 31905

Commandant
US Army Missile and Munitions
Center and School
ATTN: ATSK-CD-MD 1
ATTN: ATSK-DT-MU-EOD 1
Redstone Arsenal, AL 35809

Commander
US Army Logistics Center
ATTN: ATCL-MG 1
Fort Lee, VA 23801

Commandant
USAMP&CS/TC&FM
ATTN: ATZN-CM-CDM 1
Fort McClellan, AL 36205

Commander
US Army Infantry Center
ATTN: ATSH-CD-MS-C 1
Fort Benning, GA 31905

Commander
US Army Infantry Center
Directorate of Plans & Training
ATTN: ATZB-DPT-PO-NBC 1
Fort Benning, GA 31905

Commander
USA Training and Doctrine Command
ATTN: ATCD-Z 1
Fort Monroe, VA 23651

Commander
USA Combined Arms Center and
Fort Leavenworth
ATTN: ATZL-CA-COG 1
ATTN: ATZL-CAM-IM 1
Fort Leavenworth, KS 66027

Commander
US Army TRADOC System Analysis
Activity
ATTN: ATAA-SL 1
White Sands Missile Range, NM 88002

US ARMY TEST & EVALUATION COMMAND

Commander
US Army Test & Evaluation Command
ATTN: DRSTE-CM-F 1
Aberdeen Proving Ground, MD 21005

DEPARTMENT OF THE NAVY

Commander
Naval Explosive Ordnance Disposal
Facility
ATTN: Army Chemical Officer
Code AC-3 1
Indian Head, MD 20640

Chief, Bureau of Medicine & Surgery
Department of the Navy
ATTN: MED 3C33 1
Washington, DC 20372

Commander
Naval Weapons Center
ATTN: Technical Library
Code 343 1
China Lake, CA 93555

US MARINE CORPS

Director, Development Center
Marine Corps Development and
Education Command
ATTN: Fire Power Division 1
Quantico, VA 22134

DEPARTMENT OF THE AIR FORCE

HQ Foreign Technology Division
(AFSC)
ATTN: TQTR 1
Wright-Patterson AFB, OH 45433

HQ AFLC/LOWMM 1
Wright-Patterson AFB, OH 45433

HQ AFISC/SEV 1
Norton AFB, CA 92409

NORAD Combat Operations Center
ATTN: DOUN 1
Cheyenne Mtn Complex, CO 80914

Air Force Aerospace Medical Research
Laboratory
ATTN: AFAMRL/HE
Dr. C.R. Replogle 1
Wright-Patterson AFB, OH 45433

HQ AFTEC/SGB 1
Kirtland AFB, NM 87117

OUTSIDE AGENCIES

Battelle, Columbus Laboratories
ATTN: TACTEC 1
505 King Avenue
Columbus, OH 43201

Toxicology Information Center,
WG 1008
National Research Council 1
2101 Constitution Ave., NW
Washington, DC 20418

US Public Health Service
Center for Disease Control
ATTN: Lewis Webb, Jr. 1
Building 4, Room 232
Atlanta, GA 30333

Director
Central Intelligence Agency
ATTN: ORD/DD/S&T 1
Washington, DC 20505

ADDITIONAL ADDRESSEE

Commander
US Army Environmental Hygiene
Agency
ATTN: Librarian, Bldg 2100 1
Aberdeen Proving Ground, MD 21010

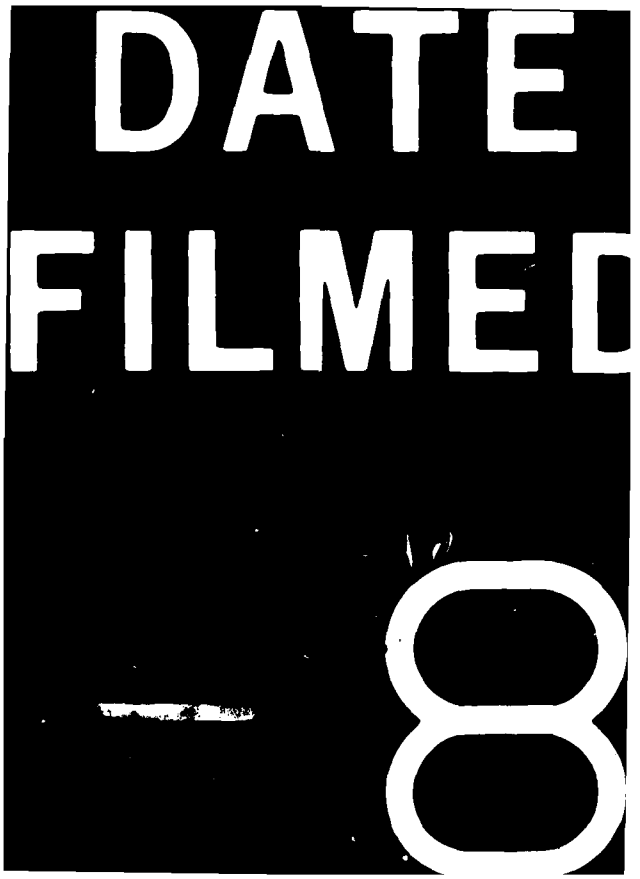
DATE
FILMED
8